SCIENCE CHINA
Technological Sciences

November 2011 Vol.54 No.11: 2854–2868
doi: 10.1007/s11431-011-4505-y

Simulation analysis theory and experimental verification of air-cushion isolation control of high concrete dams

LIU HaoWu[1, 2*], ZHANG ShaoJie[1], CHEN Jiang[1], SUN Man[3], SUN Lei[4] & LI Yi[1]

[1] *College of Hydraulic and Hydrauelectric Engineering, Sichuan University, Chengdu 610065, China;*
[2] *State Key Laboratory of Hydraulics and Mountain River Engineering, Sichuan University, Chengdu 610065, China;*
[3] *College of Electric and Information, Sichuan University, Chengdu 610065, China;*
[4] *Nuclear Power Institute of China, Chengdu 610072, China*

Received March 1, 2011; accepted June 20, 2011; published online August 11, 2011

To focus on the key scientific problem of process control of dynamic catastrophe of high dams, presented for the first time are the modelling theory of liquid-gas-solid tri-phase coupling of the air-cushion isolation control of high dams and its numerical simulation method, and theoretical description of the complicated dynamics problem of the tri-phase coupling-thermodynamics state-material-contact bi-nonlinearity, as well as the simulation analysis of the key effects of dynamic catastrophe of the air-cushion isolated high dam engineering. The analytic solution of plane-wave with rigid-dam body was created. The simulation comparison of dynamic catastrophe processes of 305 m Jinping arch dam with and without seismic control was carried out, and the results were basically in agreement with that obtained from the large shaking table tests, and verify each other. The entire air-chamber and optimized air-cushion with varying thickness were presented to develop a optimization method. The large shaking table tests of the isolated dam model, which is satisfied with the basic dynamic similarity relations, were performed for the first time. The test data seemed to be convincing and were in agreement with the dynamic simulation results of the tested model, thereby providing an experimental verification to the simulation theory and method. The combination experiments of theoretical model and physical model demonstrated that the hydrodynamic pressure of high arch dams can be reduced by more than 70% as well as the first and third principle stresses of the dam body reduced by more than 20%–30%, thereby the global anti-seismic capacity of the high dam being improved significantly. The results have shown that the air-cushion isolation is the prior developing direction of structural control technology of high concrete dams.

air-cushion isolation of high concrete dam, liquid-gas-solid multi-field coupling, material-geometry bi-nonlinearity, large shaking table test, hydrodynamic pressure

Citation: Liu H W, Zhang S J, Chen J, et al. Simulation analysis theory and experimental verification of air-cushion isolation control of high concrete dams. Sci China Tech Sci, 2011, 54: 2854–2868, doi: 10.1007/s11431-011-4505-y

1 Introduction

The dynamic control as one of modern technologies has been used more and more in the structure engineering such as building and bridge and has shown its practical effects in some strong earthquake events. It has become a modern development approach of antiseismic engineering.

However, in the field of large dam engineering, the anti-seismic control technology now remains in its early stage because of the particularity of high arch dams such as their peculiar structure and supper dimensions. As the traditional antiseismic measures, the anti-seismic reinforcing steel bars

*Corresponding author (email: liuhaowu35@yahoo.com.cn)

typically are employed, for example, two-dimensional antiseismic reinforcement was adopted in the 271 m high Inguri arch dam in USSR. The expenses of the steel bars amounted to 23.9 kt and cost was great. Hence, it is an urgent and challenging problem to develop an effective and feasible control principle and technology.

Types of dams' antiseismic control. There are mainly two kinds of aseismic control principles and technologies, which are now used in the building-bridge engineering: isolation, energy dissipation. Recently, the damper was used in the Retello dam, Italy. The dampers used in arch dams may produce hysteretic energy dissipation by means of the opening of the contraction joints during strong earthquakes [1]. The related study shows that there are two difficult points in application of dampers to the high dam control.

- Small displacement and energy dissipation. The opening value of the contraction joints of high arch dams is only in the order of 10 mm, which is smaller than that in the bridges or buildings by 1–2 orders of magnitude. Therefore, dampers' hysteretic energy dissipation is very little. Thereby, for the huge dam body, "the improvement of dam stress state is extremely weak" [1], and "their influence on the dam's seismic response is utterly limited" [2].
- Risk of estimation of the contraction joint opening. According to the typical computation model, all the contraction joints will open, in fact, however, joint opening mainly occurred at one contraction joint in practical earthquakes. Up to now, three events of contraction joint opening of arch dams occurred, including 2 events (1971, 1944) at the 113 m high Pocaima arch dam, USA, and another one (1999) at Guguan arch dam (Taiwan, China). According to the analysis results, the maximum opening will occur at the crown; however, practical maximum opening in the three events mentioned above occurred at near the dam abutment. As a result, if the dampers are installed at each joint, most of them will be no more displacement or energy dissipation; if dampers installed concentrative, it is difficult to estimate where the opening will occur.

Because of the peculiarity of the dams, which carry bi-direction loads, the realization approach of seismic isolation for dams is different from the base isolation used for buildings. The isolation interface is located on the upstream face of the dams instead of at the base for buildings; and the isolation device is air-cushion instead of rubber bearing. In sum, as a soft wave filter layer, the air-cushion realizes aseismic control of dams by isolating dams from the dynamic pressure generated in the water during earthquake.

In fact, the air-cushion surge chamber used in the hydroelectric power station is well known. Here the air cushion is used just to reduce dynamic pressures generated by the water hammer instead of by the earthquake.

Indeed, the values of air-cushion isolation to the antiseismic safety of arch dams depend on the ratio of the hydrodynamic pressure to dams' total seismic load. According to the field excitation test of three arch dams (113 m Monticcello (USA), 110 m Shataya (Japan), 186 m Kurobe 4 (Japan)) and 3D FEM analysis of two arch dams (240 Ertan, 278 m Xiluodu), the ratios of dams' mass to added mass of hydrodynamic effects are 1:2.52, 1:4.69, 1:1.34, 1:0.87, and 1:0.80, respectively. It follows that the hydrodynamic pressure amounts to about half of the total seismic loads for the arch dams in the order of 200–300 m height. Therefore, the air cushion furnishes an effective solution of the aseismic safety problem of high arch dams provided that it is able to reduce dynamic pressures significantly.

Development of aseismic air-cushion technology of dams. Starting from the 1950s, the studies were made to develop the aseismic air-cushion of dams in France, USSR etc. The prototype test was performed on the 20 m high Klivobolouri gravity dam, USSR, using blasting exciting. The dynamic pressures were reduced by 67%–88% [3, 4]. However, the frequency of the dam and the impact wave in the water were too high (13–23 Hz), which was not suitable for the high dams. In the 1980s, the air-cushion was employed in two arch dams, i.e., 232 m Chirkey dam and 86 m Miatly dam in the USSR [5, 6]. In the 1990s, the air-cushion was adopted by design of the 155 m high Mok gravity dam in the Russia, with the results that its section decreased by 9% and the benefit was great [4].

The gas with normal pressure in the air-cushion relies on the air compressor and the air supply pipe system. The practical experiments obtained from the air-cushion surge chamber of hydroelectric power station have shown that air leak of the surge chamber is small. As a typical example, the air leakage from the air-cushion surge chamber with a volume of 110000 m^3 of the Kvilldal hydroelectric power station, Norway, whose air-cushion chamber is the biggest one in the world, is only 0.17 nm^3/min. In addition, its electricity consumption is 547000 kW·h per year in multi-year average. It follows that the air supply and pressure maintenance for dams' air-cushion seem feasible.

The restricted factors of application of the aseismic air-cushion to dams mainly are (i) some appurtenant structures and equipments will located on the upstream surface of dams; (ii) reservoir sedimentation. These factors will confine the installation range of the aseismic air cushion.

Analysis theory and model experiment of air-cushion isolation control. As for the theory, the dam with air-cushion was simplified as a single-degree system and analyzed in the USSR; Hall et al. [7] performed a linear 2D FEM analysis of a gravity dam with the gas-filled balloon or bubble air cushion; Li [8] studied the gas-filled balloon isolation of a 2D rigid gravity dam based on potential theory of incompressible fluid. The theory of the dams' air-cushion isolation is a problem of the fluid-solid coupling dynamics. However, the general theory and its numerical implement method have almost not been presented for a long time [9].

In recent years, the research on the both of numerical model and physical model has been taken in China, and a dynamic 3D FEM of the liquid-gas-solid coupling and

computation examples of 190.5 m Longtan gravity dam, Xiluodu and Jinping arch dams [10–13], as well as shaking table model tests of Longtan dam and Jinping dam carried out [12, 13]; their results showed that dynamic pressures could be reduced by more than 60%.

These investigations pioneered the 3D analysis of liquid-gas-solid coupling and the shaking table dynamic model tests. They were important and demonstrated the development approach of R & D based on the up-to-date scientific disciplines. However, there were some important limitations including mainly: as to the theory, (i) in the theoretical model, the state equation and the thermodynamics characteristic of the gas were not involved, (ii) in the structure simulation, the contact problem of contraction joint opening and the geometry nonlinearity were not considered; as for the test, (i) the air chambers were discrete and did not form a complete isolation cushion in the model, (ii) the air chambers were made from organic glass plate and did not satisfy the similarity relations exactly, (iii) the dynamic elastic modulus of materials of the dam model also did not meet the similarity relations perfectly. These questions led to some errors in the theoretical analysis results and in the model test data.

This paper is intended to report the focal leap and effective breakthrough obtained by the research on the high dams' aseismic control, which utilizes the experiment media of a combination of the numerical model and the physical model to study systematically study the principle and technology of the dams' aseismic air-cushion control and to implement the entire process simulation of aseismic mechanisms and control optimization as well as shaking table tests, considering the multi-phase coupling-thermodynamics characteristics and material-geometry bi-nonlinearity. These results are possessed of important theoretical significances and high practical application values to engineering.

2 Modeling theory and numerical implement method of air-cushion isolation control of high dams

2.1 Modeling theory of air-cushion isolation of high dams

The dynamic system of the air-cushion isolated dams consists of four subsystems, namely dam body, air cushion, water reservoir, and dam foundation (shown in Figure 1). It is a complicated multi-field strong coupling dynamic system. In the dynamics theory, it may be summarized as a problem of liquid-gas-solid tri-phase coupling.

The dynamic behaviour and seismic catastrophe process of the dam structure-isolation air-cushion system include two basic states: (i) elastic state without any damage; (ii) elastic-plastic state with some dynamic damages. Accordingly, the two key effects, which determine the dynamic behaviour and catastrophe process of high dams' liquid-gas-solid tri-phase systems are: firstly, the nonlinear dynamic coupling effects of material-structure-environment, especially the strong nonlinear coupling between liquid-solid system and the confined gas, which possesses the peculiarity of negative stiffness and the complexity of coupling of the structure and environment; secondly, the dynamic contact nonlinearity of seismic catastrophe, especially the contraction joint opening-closing, and its superposition with the material nonlinearity.

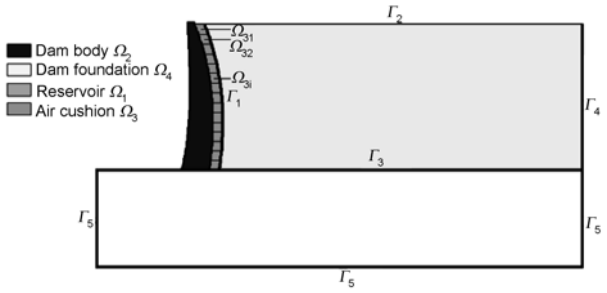

Figure 1 Schematic of the reservoir, air cushion, dam body and dam foundation dynamic system.

In the theoretical description of dynamics behaviour of these subsystems in the elastic state, the solid region (dam-foundation) is described by the small deformation elastic theory and the liquid region (reservoir water) by the wave equation; as to the gas region (air-cushion), it is just the difficult point and special question of the theoretical description of the tri-phase coupling system.

The air filled in the air-cushion, whose viscosity is extremely small, may be considered as an ideal gas. Its motion equation under the condition of small disturb is

$$\frac{1}{c^2}\ddot{p} - \nabla p = 0, \tag{1}$$

where p is pressure, and c is the sound velocity.

The state equation (constitutive equation) is expressed by the gas thermodynamics equation as

$$pV^{\gamma} = \text{const}, \tag{2}$$

where V is the volume, and γ is the ratio of specific thermal capacity (γ=1.0 in the isothermal process, γ=1.4 in the isentropic process).

The operation and monitoring of air-cushion surge chambers in Norway etc. indicate that the air-cushion surge chambers behave in an adiabatic state during water hammer (2–3 min). The duration of earthquakes is shorter than that of water hammer. Thus, the dam air-cushion behaves in an adiabatic process during earthquakes.

In summary, by combining the wave equation and state equation of the gas with the corresponding governing equations of the liquid and solid, the governing (partial differential) equation group of the liquid-gas-solid tri-phase dynamic coupling is established. The given accessory condi-

tions for a solution of the basic equations include the initial conditions and the boundary conditions, especially the fluid-solid coupling conditions and the viscous-spring artificial condition expressing the radiation damping of foundation, namely,

Coupling conditions at water-gas interface:

$$p\,|_i = p_w\,|_i;\ \ u^n\,|_i = u_w^n\,|_i\ . \tag{3}$$

Coupling conditions at gas-dam interface:

$$u^n\,|_i = u_d^n\,|_i;\ \ \frac{\partial p}{\partial n} = -p\ddot{u}_n, \tag{4}$$

where p_w is water pressure, subscript i denotes the interface, n denotes normal direction, u_n is the normal displacement, subscript w denotes the water and d denotes the dam body. Boundary conditions of the gas:

$$p=0 \text{ (on the top of air-cushion);} \tag{5a}$$

$$\frac{\partial p}{\partial n} = 0 \quad \text{(on the bottom of the air-cushion).} \tag{5b}$$

Boundary conditions of the reservoir:

$$p=0 \text{ (ignoring effects of surface wave),} \tag{6a}$$

$$\frac{\partial p}{\partial n} = -\frac{\beta}{c}\dot{p} \text{ (on the bottom of reservoir),} \tag{6b}$$

$$\frac{\partial p}{\partial n} = -\frac{1}{c}\dot{p} \text{ (on the tail of reservoir),} \tag{6c}$$

where β is the reservoir bottom absorption coefficient, and $0 \leqslant \beta \leqslant 1$.

The viscous-spring artificial boundary conditions of the computation region of dam foundation [16]:

$$\begin{cases} \text{For } P \text{ wave: } K_p = A\dfrac{E}{2r_f},\ \ D_p = \rho \cdot c_p \cdot A, \\ \text{For } S \text{ wave: } K_s = A\dfrac{G}{2r_f},\ \ D_s = \rho \cdot c_s \cdot A, \end{cases} \tag{7}$$

where K_p and K_s are the spring stiffness coefficients of P wave and S wave, respectively; D_p and D_s are damping coefficients of dampers of P wave and S wave, respectively; E and G are the elastic modulus and shear modulus, respectively; ρ is the mass density; C_p and C_s are the velocities of P wave and S wave, respectively; A is the influencing area of mesh nodes in free field; r_f is distance between the scattering source and artificial boundary.

2.2 Analytic solution of air-cushion isolation for the rigid dam

The liquid-gas-solid coupling equations mentioned above are extremely complicated. Its analytic solution was obtained under the following simple conditions for the first time in refs. [11, 13]: (i) rigid dam body with vertical upstream face, (ii) infinite length of dam body and reservoir, (iii) constant thickness of the air-cushion and zeros stress gradient in the air-cushion along the vertical direction. This situation is similar to a long gravity dam with vertical upstream face, long reservoir and the large stiffness of the dam foundation.

In this case, the wave eq. (1) can be simplified as follows:

$$\frac{\partial^2 p}{\partial x^2} - \frac{1}{c^2}\frac{\partial^2 p}{\partial t^2} = 0, \tag{8}$$

where x is the horizontal coordinate (the upstream face of the dam taken as the zero point), and t is the time.

Eq. (8) shows that any perturbation in the reservoir and the air-cushion will produce plane waves with the same regularity. Since the Fourier series can express any wave, here the basic situation with the harmonic wave as the input motion is solved. Let the harmonic wave be

$$\ddot{u}_g(t) = \ddot{u}_0 \mathrm{e}^{i\omega t}, \tag{9}$$

where $\ddot{u}_g$ is the acceleration of the dam foundation. So the solution of eq. (8) is

$$\begin{cases} p = (A\mathrm{e}^{-\mathrm{i}kx} + B\mathrm{e}^{\mathrm{i}kx})\mathrm{e}^{\mathrm{i}\omega t} \text{ (air-cushion),} \\ p_w = A_1\mathrm{e}^{-\mathrm{i}k_w(x-b_0)}\mathrm{e}^{\mathrm{i}\omega t} \text{ (reservoir),} \end{cases} \tag{10}$$

where A, B, A_1 are the undetermined coefficients, ω is the circular frequency, b is the thickness of the air-cushion, $k=\omega/c$, and $k_w=\omega_w/c_w$.

According to eqs. (3) and (4), the coupling conditions can be shown as follows

$$p\big|_{x=b} = p_w\big|_{x=b};\ u\big|_{x=b} = u_w\big|_{x=b};\ \frac{\partial p}{\partial n} = -p\ddot{u}_n. \tag{11}$$

The amplitude of the hydrodynamic pressure on the upstream face of the dam can be obtained.

$$\|p\|_{x=0} = \frac{\rho c \ddot{u}_g}{\omega}\left\|\frac{(R_0-1)-\mathrm{e}^{2\mathrm{i}kb}(R_0+1)}{R_0(1+\mathrm{e}^{2\mathrm{i}kb})+(\mathrm{e}^{2\mathrm{i}kb}-1)}\right\|, \tag{12}$$

where R_0 is the damping ratio of the air-cushion to the reservoir, and $R_0=\rho c/\rho_w c_w$.

The analytic solution shows the relationships between the hydrodynamic pressure and the thickness b of the air-cushion as well as the exciting frequency ω in the condition of the rigid dam.

Obviously, the thickness of the air-cushion has noticeable effects on the decreasing amplitude of the hydrodynamic pressure. However, when it is relatively thick, the marginal utility will occur. Namely, the efficiency of increasing the thickness will decrease. Moreover, frequency is another main influencing factor of the isolation effect. In the ad-

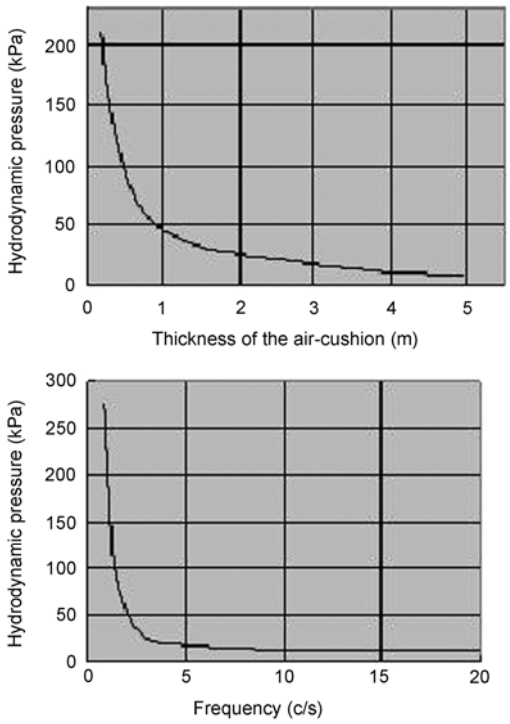

Figure 2 Relation curves of the hydrodynamic pressure to thickness of the air-cushion and the exiting frequency.

vantage frequency range (1–8 Hz) of the earthquake wave, very good isolation effect can be obtained.

2.3 Numerical implementation method of the theoretical analysis model of air-cushion control of high arch dam

In the view of the complexity of the high dam engineering and strong nonlinearity of the mechanical behaviour of the air-cushion, the global-field finite element method is adopted to simulate the liquid-gas-solid dynamic coupling system of the seismic control of the high dam. Namely, the FEM is used for the fields of liquid phase, gas phase and solid phase, respectively.

Gas element mode. As for the liquid-gas-solid dynamic coupling system, the air phase is the key difficulty compared to the usual fluid-solid coupling problem.

At the beginning of the earthquake (t=0), the gas in the air-cushion is in the static state. The static gas pressure at the arbitrary depth of the reservoir at this moment is denoted by P_0, the bulk modulus of the ideal gas element can be obtained from the derivation of eq. (2) [22]:

$$K = -\gamma p^{1+\frac{1}{\gamma}} / p_0^{\frac{1}{\gamma}}, \tag{13}$$

where p (p=p(t)) is the gas pressure at arbitrary time.

It can be readily seen that the expression of peculiarity of mechanical behaviour for the gas contained within the air-cushion includes nonlinearity, variable rigidity, and negative rigidity. Therefore, it is of great difficulty to numerically simulate.

As known, the Lagrange coordinate system is usually adopted in the solid mechanics and the Euler coordinate system in the fluid mechanics. Herein, the skill and characteristic of formulation of the simulation algorithm for the tri-phase liquid-gas-solid dynamic coupling are that the Euler method is used in the liquid phase, and the pressure is taken as the field variable; the Lagrange method used in the gas phase, and the displacement taken as the field variable. Then, the harmonious condition of displacement at the interface of the air cushion-dam body can be automatically satisfied. So the mechanical constitutive relation of the air-cushion (shown in eq. (14)) based on the displacement formulation in Lagrange method is presented to overcome the spurious zero-energy mode and singularity of the air-cushion in numerical computation as follows:

$$\begin{Bmatrix} \boldsymbol{\varepsilon}_V \\ \boldsymbol{\gamma}_{xy} \\ \boldsymbol{\gamma}_{yz} \\ \boldsymbol{\gamma}_{xz} \\ \boldsymbol{\theta}_x \\ \boldsymbol{\theta}_y \\ \boldsymbol{\theta}_z \end{Bmatrix} = \begin{bmatrix} 1/\boldsymbol{K} & 0 & 0 & 0 & 0 & 0 & 0 \\ 0 & \boldsymbol{C}_s & 0 & 0 & 0 & 0 & 0 \\ 0 & 0 & \boldsymbol{C}_s & 0 & 0 & 0 & 0 \\ 0 & 0 & 0 & \boldsymbol{C}_s & 0 & 0 & 0 \\ 0 & 0 & 0 & 0 & \boldsymbol{C}_r & 0 & 0 \\ 0 & 0 & 0 & 0 & 0 & \boldsymbol{C}_r & 0 \\ 0 & 0 & 0 & 0 & 0 & 0 & \boldsymbol{C}_r \end{bmatrix} \begin{Bmatrix} \boldsymbol{p} \\ \boldsymbol{\tau}_{xy} \\ \boldsymbol{\tau}_{yz} \\ \boldsymbol{\tau}_{xz} \\ \boldsymbol{M}_x \\ \boldsymbol{M}_y \\ \boldsymbol{M}_z \end{Bmatrix}, \tag{14}$$

where ε_v is the bulk strain, K is the bulk modulus, γ_{ij} is the shear strain, τ_{ij} is the shear stress, θ_i is the rotation about axis i, C_s and C_r are the constraint parameters of the shear and rotational stability, respectively, p is the gas pressure, and M_i is the twisting force about axis i.

The tri-phase dynamic coupling system has the properties of the nonlinearity and leads to the failure of the deformation-superposition method. So the increment dynamic method of global-field solution is adopted for the dynamic analysis. The step-by-step integration method is used in the time domain, and the increment of the element volume ΔV can induce the corresponding increment of the gas pressure Δp in each time step:

$$\Delta p = \gamma p_s \frac{\Delta V}{V_s}. \tag{15}$$

Eq. (15) is the increment equation of the gas element.

Obviously, herein the bulk modulus of the gas in the air-cushion element is determined by itself ignoring the structural effects of isolation RC plate between air and water, because the plate is very thin, say $\approx$ 0.2 m, whose bending stiffness is only 1×10^{-7} of that of the dam body (average thickness = 35.5 m).

Motion equation of the liquid-gas-solid tri-phase system. The Galekin's method is used for discretizing fluid-solid coupling equation after introducing some corresponding boundary conditions, by which the dynamic bal-

ance equation of reservoir-air cushion-dam body-dam foundation can be obtained as follows:

$$\begin{bmatrix} \boldsymbol{M}_s & 0 \\ \boldsymbol{\rho R}_l & \boldsymbol{M}_l \end{bmatrix} \begin{Bmatrix} \ddot{\boldsymbol{u}} \\ \ddot{\boldsymbol{p}}^e \end{Bmatrix} + \begin{bmatrix} \boldsymbol{C}_s & 0 \\ 0 & \boldsymbol{C}_l \end{bmatrix} \begin{Bmatrix} \dot{\boldsymbol{u}} \\ \dot{\boldsymbol{p}}^e \end{Bmatrix} + \begin{bmatrix} \boldsymbol{K}_s & -\boldsymbol{R}_l^T \\ 0 & \boldsymbol{K}_l \end{bmatrix} \begin{Bmatrix} \boldsymbol{u} \\ \boldsymbol{p}^e \end{Bmatrix} = \begin{Bmatrix} \boldsymbol{f} \\ 0 \end{Bmatrix}, \tag{16}$$

where $[\boldsymbol{M}_s]$, $[\boldsymbol{C}_s]$ and $[\boldsymbol{K}_s]$ are mass, damping and stiffness matrices of dam body-foundation-air cushion, respectively; $[\boldsymbol{M}_l]$, $[\boldsymbol{C}_l]$ and $[\boldsymbol{K}_l]$ are the mass, damping and stiffness matrices of the reservoir; $\{\boldsymbol{R}_l\}$ is the coupling matrix of the interface of the reservoir-air cushion; $\{\boldsymbol{f}_l\}$ is the load vector of the interface of the reservoir-air cushion; $\{\boldsymbol{f}\}$ is the outside excitation except the load vector $\{\boldsymbol{f}_l\}$; $\{\boldsymbol{p}^e\}$ and $\{\ddot{\boldsymbol{u}}\}$ are the pressure vector and acceleration vector of element nodes, respectively. In addition

$$[\boldsymbol{M}_l] = \frac{1}{\boldsymbol{c}^2} \iiint_{\Omega_w} \boldsymbol{N}\boldsymbol{N}^{\mathrm{T}} \mathrm{d}\boldsymbol{v} + \frac{1}{\boldsymbol{g}} \iint_{\Gamma_2} \boldsymbol{N}\boldsymbol{N}^{\mathrm{T}} \mathrm{d}\boldsymbol{S}, \tag{17}$$

$$[\boldsymbol{C}_l] = \frac{\boldsymbol{\beta}}{\boldsymbol{c}} \iiint_{\Gamma_3} \{\boldsymbol{N}\}\{\boldsymbol{N}\}^{\mathrm{T}} \mathrm{d}\boldsymbol{S} + \frac{1}{\boldsymbol{c}} \iint_{\Gamma_4} \{\boldsymbol{N}\}\{\boldsymbol{N}\}^{\mathrm{T}} \mathrm{d}\boldsymbol{S}, \tag{18}$$

$$[\boldsymbol{K}_l] = \iiint_{\Omega} [\boldsymbol{B}]^{\mathrm{T}} [\boldsymbol{B}] \mathrm{d}\boldsymbol{v};\ [\boldsymbol{B}] = \{\boldsymbol{L}\}\{\boldsymbol{N}\}^{\mathrm{T}}, \tag{19}$$

$$\{\boldsymbol{L}\}^{\mathrm{T}} = \begin{bmatrix} \dfrac{\partial}{\partial x} & \dfrac{\partial}{\partial y} & \dfrac{\partial}{\partial z} \end{bmatrix}, \tag{20}$$

$$[\boldsymbol{R}_l] = \iint_{\Gamma_1} \{\boldsymbol{N}\}\{\boldsymbol{N}_s\}^{\mathrm{T}} [\boldsymbol{\Lambda}] \mathrm{d}\boldsymbol{S};\ \{\boldsymbol{f}_l\} = [\boldsymbol{R}_l]^{\mathrm{T}} \{\boldsymbol{p}^e\}, \tag{21}$$

where $\{\boldsymbol{N}\}$ is the interpolation function vector of pressure, $\{\boldsymbol{N}_s\}$ the interpolation function vector of displacement; Ω_w is the spatial domain of the reservoir; Γ_1, Γ_2, Γ_3 and Γ_4 are the interface of the reservoir-air cushion, the free surface of the reservoir, the bottom of the reservoir, the tail of the reservoir, respectively.

2.4 Modeling theory and its numerical method of the catastrophe damage contact nonlinearity of air cushion control of high dam

So far, three simulating analysis theories of the arch dam dynamic damage have been presented as follows.

1) The elastic-plastic analysis method based on the continuum damage mechanics [17].

2) The elastic-plastic model based on the Drucker-Prager yield criterion [18].

3) The analysis method of geometrical nonlinearity based on the contact theory [19].

The first two methods both base themselves on a basic assumption that the dam body is homogeneous, isotropy and consists of integral materials. However, this assumption is inconsistent with the realities of the arch dam engineering. In fact, a number of contraction joints are usually arranged within the arch dam body and thereby becomes a series of weak vertical interfaces of the dam body due to whose low tensile strength (the tensile strength of the contraction joint is less than 0.1 times the strength of the concrete)

The earthquake damages and research related have shown that the strong earthquake may cause the opening closing of the contraction joint and this opened joint becomes the uncontinuity interface, and leads to redistribution of dam-body stresses both in the arch and cantilever directions [19, 20], and thereby the dynamic response and aseismic safety of arch dams must be influenced severely. Thus, a key effect of the dynamic damage of earthquakes on the arch dam is the geometry nonlinearity, i.e., the dynamic contact nonlinearity effect.

The mechanical description of the contact surface of the contraction joints based on the Coulomb theory is shown as follows:

$$\tau_{\lim} = \mu N + d;\quad \tau_{\lim} \leqslant \tau_{\max}, \tag{22}$$

where $\tau_{\lim}$ is the equivalent shear stress, d is the cohesive force, μ is the friction coefficient, N is the normal pressure, $\tau_{\max}$ is the maximum shear stress that the contact surface can resist. Its value is assumed to be 10^{20} Pa.

The basic contact equation is well known, and the augmented Lagrange method is adopted in this simulation analysis. Its corresponding normal-pressure formula on the contact surface can be expressed as follows:

$$\begin{aligned} N &= \begin{cases} K_n u_n + \lambda_{i+1}, & u_n \leqslant 0, \\ 0, & u_n > 0, \end{cases} \\ \lambda_{i+1} &= \begin{cases} K_n' u_n + \lambda_i, & |u_n| > \varepsilon, \\ \lambda_i, & |u_n| < \varepsilon, \end{cases} \end{aligned} \tag{23}$$

where K_n is the normal stiffness, u_n is the normal displacement (opening is positive) between contact surfaces, λ_i is the Lagrange iteration multiplier, and ε is the tolerance.

2.5 Numerical simulation example of high arch dam engineering survey, computation model and condition

The Yalong River Jinping first stage hydropower station is located in Yanyuan county, Sichuan province, China. The dam of the hydropower station is a concrete double curvature arch dam, whose thickness at the crown section varies from 13 m at the crest (elevation of 1885 m) to 58 m at the base. It is a thin arch dam with the ratio 0.19 of thickness to height. The designed installed capacity of this hydropower station is 3300 MW, whose annual average power output is 16.6×10^9 kW·h and the capacity of the reservoir is 7.76 billion m^3. The normal storage level and low operation water level of the hydropower station are 1880 m, and 1800 m, respectively. This 305 m dam is the highest arch dam presently under construction in the world.

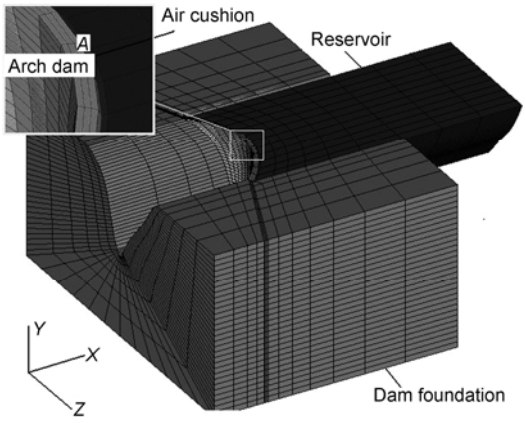

Figure 3 Finite element model of the dam-aircushion-reservoir coupling system.

The 3D finite element model meshed with 8-node tetrahedral solid element is shown in Figure 3.

Its total number of the nodes is 15262, when the thickness of the air-cushion is 3 m. The calculated region of the FEM is shown as follows: the limit of the dam foundation is 1000 m× 700 m× 1200 m, the length of reservoir is 3 times the height of the dam. In this FEM, the boundary condition of fluid-solid coupling is set on the interface of the air cushion-reservoir, reservoir-dam foundation, respectively; the infinity boundary condition is set on the end of the reservoir; the effects of the surface wave are not considered; as the sediment charge of the Yalong river is very small and its mean annual sediment charge is only 0.45 kg/m^3, the hydrodynamic wave absorption at the reservoir boundary is ignored.

In the FEM, the 13 contraction joints and their opening as well as contact nonlinearity have been simulated. The 13 joints are numbered from the left bank to the right bank. The No.7 joint is located at the arch crown and the No.5 and No.10 joints are located at the quarter of the arch ring. The contact elements are set on the each contraction joint. In the simulation of the joint deformation, the joint opening-closing is considered and the slip is neglected. The reasons of this treatment method are: firstly, it is very difficult to simulate the joint keys' beveled geometries as used in the engineering practice, so up to now the modeling of bevel joint slip is unsatisfactory yet [23]; secondly, this method is used by the vast majority of researchers up to now [15, 23, 24]; finally, more important, as the unique practice example of the most severe joint damages caused by earthquakes, the opening components of Pacoima arch dam in 1971, 1994 were 9.7, 47 mm, respectively, and corresponding slip components were 0, 13.6 mm, respectively, so the slip amounted in average to only 14.4% of the opening.

The main calculated parameters for the FEM are shown as follows: for the dam foundation, its dynamic elasticity modulus, mass density and Poisson's ratio are 45 GPa, 25 kN/m^3, 0.25, respectively. True, the deformation modulus of geological formations in the left abutment is relatively low, however, the very comprehensive foundation treatment engineering has been taken, including excavation, comprehensive consolidation grouting, grout curtain, drainage, especially the concrete backfill in large-scale such as backfill tunnels, oblique walls, backfill grids etc. These treatments must increase the abutment modulus effectively. In addition, the dynamics modulus is larger than the static elastic modulus to a considerable degree.

For the dam body, its dynamic elasticity modulus, mass density and Poisson's ratio are 31.2 GPa, 24 kN/m^3, 0.167, respectively. Sound velocity and mass density of the reservoir water are 1430 m/s and 10 kN/ m^3, respectively. The density and bulk modulus of the air-cushion are established by the element center's pressure (the atmosphere pressure is considered).

All the simulation analysis cases, shown in Table 1, may be classified into the two groups, 9 kinds of cases. The first group I: as for the model of elasticity, the comparison analysis of the isolated dam (four kinds of thickness of the air-cushion) and the conventional dam (without air-cushion) is carried out; the second group II: for the elastic-plastic model, the cases of normal storage level and the operation low water level are simulated, and the comparison of the isolated dam (the air cushion with varied-thickness) and the conventional dam is completed. The earthquake waves of 1940 El Centro N-S and the 1952 Taft are chosen as the input ground motion. The calculating time of time history analysis is 20 s, time step of calculation is 0.02 s.

Results of simulation analysis. Due to limited space, the typical simulation results are shown in this paper. As for the first group I, i.e., the linear-nonlinear simulation of the arch dam-air cushion control system in its elastic state excited by the El Centro wave, the distributions of hydrodynamic pressure on the upstream surface of the dam are shown in Figure 4; the time history of hydrodynamic pressure at the crown base of the arch dam is shown in Figure 5; the peak value of the hydrodynamic pressure and its decline induced by the El Centro wave and Taft wave is shown in Table 2; the peak value of the principal stress and its reduction range shown in Table 3.

Table 1 Cases of the dynamic simulation of the air-cushion isolation for Jinping high arch dam

Dynamic state	I		Elastic state			II	Elastic-plastic state: joint opening		
Cases	I–1	I–2	I–3	I–4	I–5	II–1	II–2	II–3	II–4
Thickness of air-cushion (m)	0	1	2	3	1–2–3	0	1–2–3	0	1–2–3
Level of reservoir (m)	1880					1880		1800	

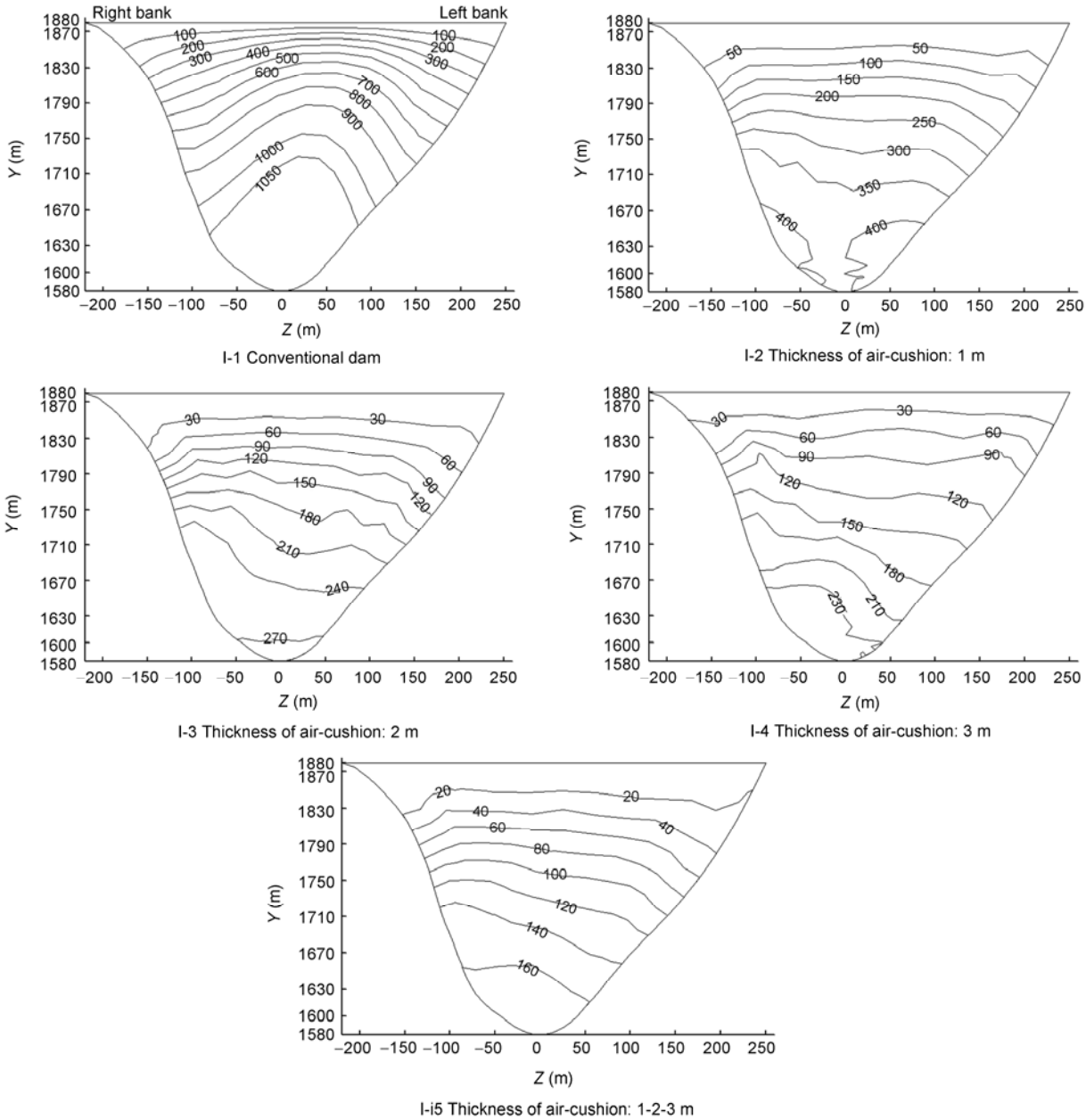

Figure 4 Comparison of hydrodynamic pressure of isolated dam with the conventional dam.

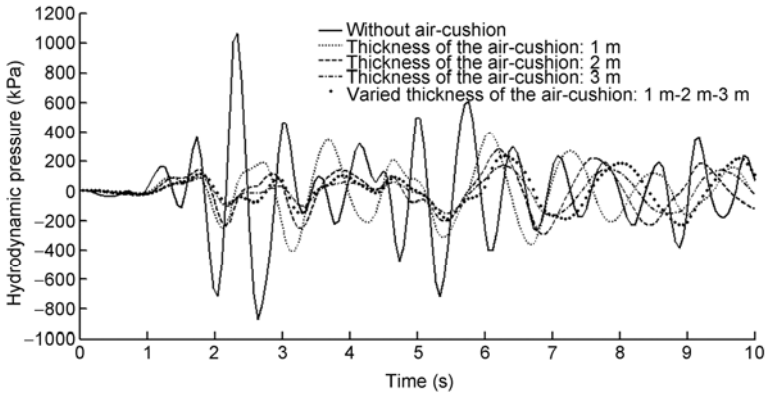

Figure 5 Time history of hydrodynamic pressure at crown base of Jinping high arch dam.

Table 2 Peak value of the hydrodynamic pressure (kPa) and reduction range on the upstream surface of the dam

Cases		I–1	I–2	I–3	I–4	I–5
Earthquake waves	El Centro	1096.6	458.7	313.0	198.1	275.9
	Reduction range (%)	0	58.2	71.5	81.9	74.8
	Taft	977.7	427.7	308.5	230.9	289.5
	Reduction range (%)	0	56.3	68.5	76.4	70.4

Table 3 Peak value of the normal principal stress (MPa) and reduction range

Cases		I–1		I–2		I–3		I–4		I–5	
Principal stress		Tens. stress	Com. stress	Tens. stress	Com. stress	Tens. stress	Com. stress	Tens. stress	Com. stress	Tens. stress	Com. stress
Earthquake wave	El Centro	7.68	–7.13	3.45	–3.85	2.99	–3.62	2.79	–3.33	2.87	–3.47
	Taft	6.24	–6.10	3.85	–3.69	3.66	–3.23	3.43	–2.88	3.58	–3.07
Reduction range (%)	El Centro			55.1	46.0	61.1	49.2	63.7	53.3	62.6	51.3
	Taft			38.3	39.5	41.3	47.0	45.0	52.8	42.6	49.7
	average			46.7	42.7	51.2	48.1	54.3	53.0	52.6	50.5

As for the second group II, the distribution of the max opening width of the contraction joints (No.5, 7, 10) of the normal storage level and operation low water level caused by the El Centro earthquake wave is shown in Figure 6; time history of opening width of contraction joints is shown in Figure 7; the opening value of typical joint and its reduction range are shown in Table 4; the time history of hydrodynamic pressure at the crown base of the arch dam is shown in Figure 8; the peak value of the hydrodynamic pressure and its decline induced by the El Centro and Taft wave is shown in Table 5; the distribution of the peak value of the first principal normal stress (tensile stress) on the upstream face of the dam is shown in Figure 9; the peak value of the first and third principal normal stress (tensile stress and compressive stress) is shown in Table 6.

Analysis of the simulation results. 1) The simulation results (hydrodynamic pressure, stress and its distribution and the opening value of the joints) of the two groups (the elastic and elastic-plastic models) are rational, which satisfy the mechanical principle and have a fairly good agreement with the conclusion of the analytical solution. The validity of the modeling theory of liquid-gas-solid coupling and

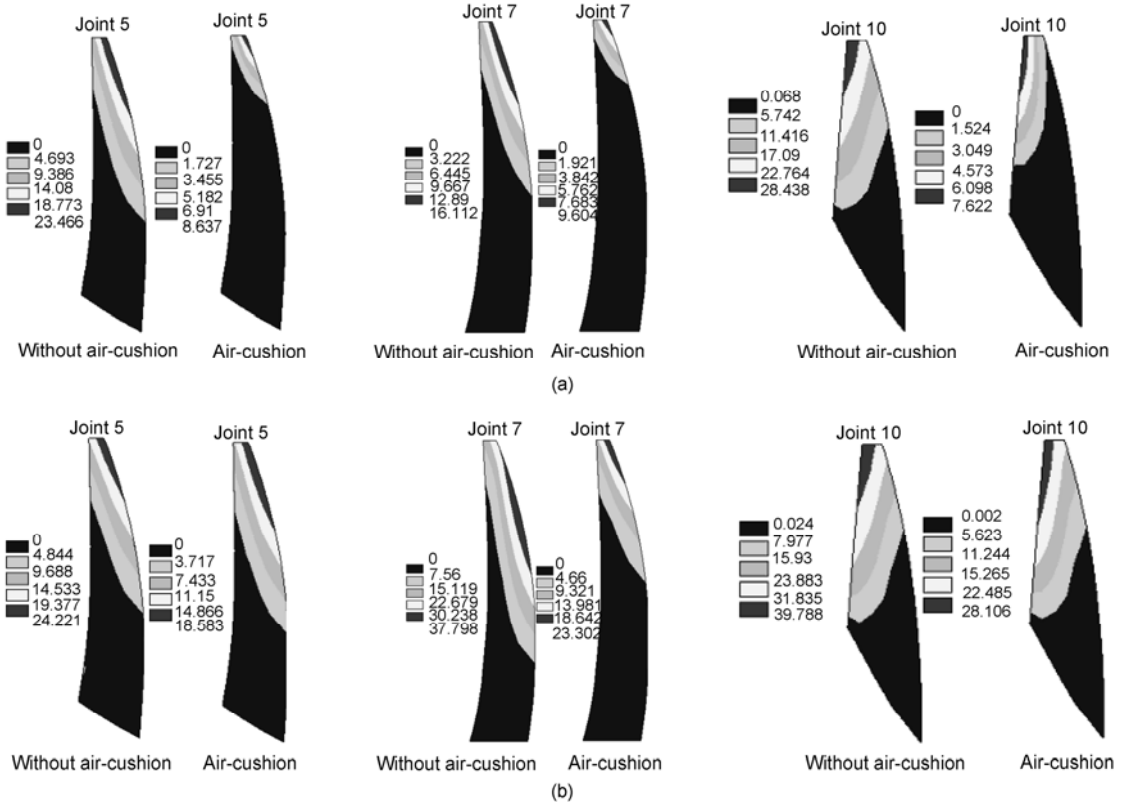

Figure 6 Comparison of the distribution of max opening value of contraction joints with air-cushion to without air-cushion (mm). (a) Normal water level; (b) low operation water level.

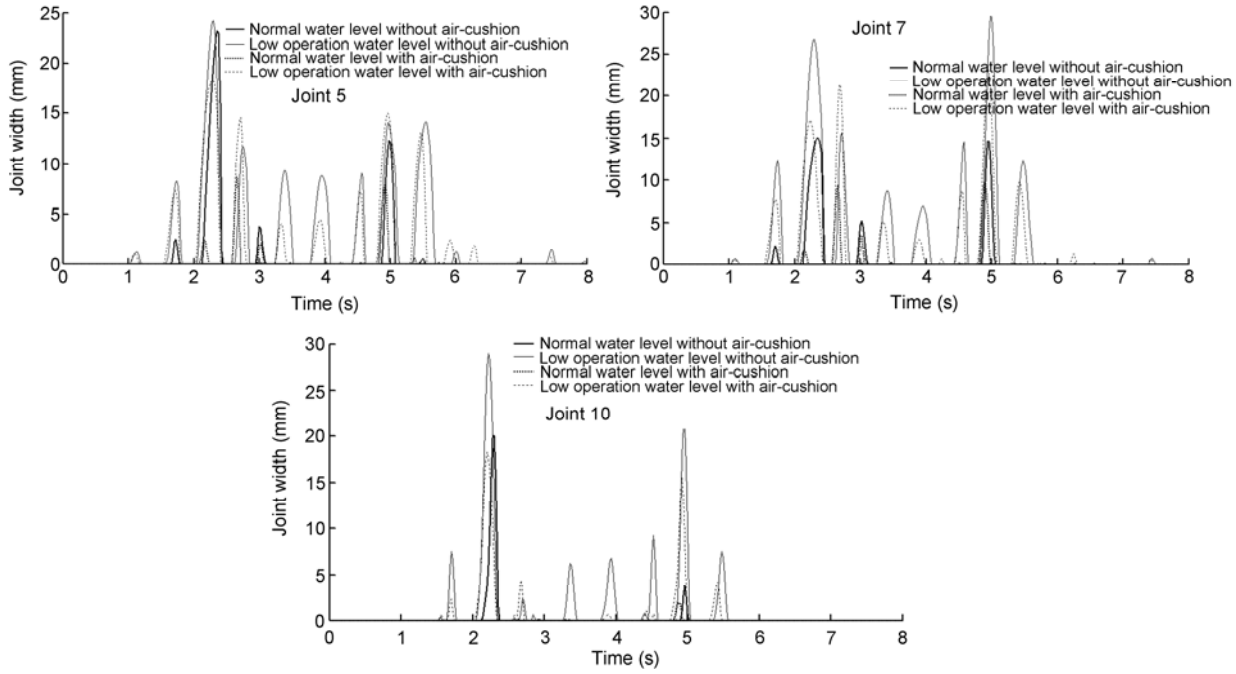

Figure 7 Comparison of the time history of the opening width of contraction joints with air-cushion to without air-cushion.

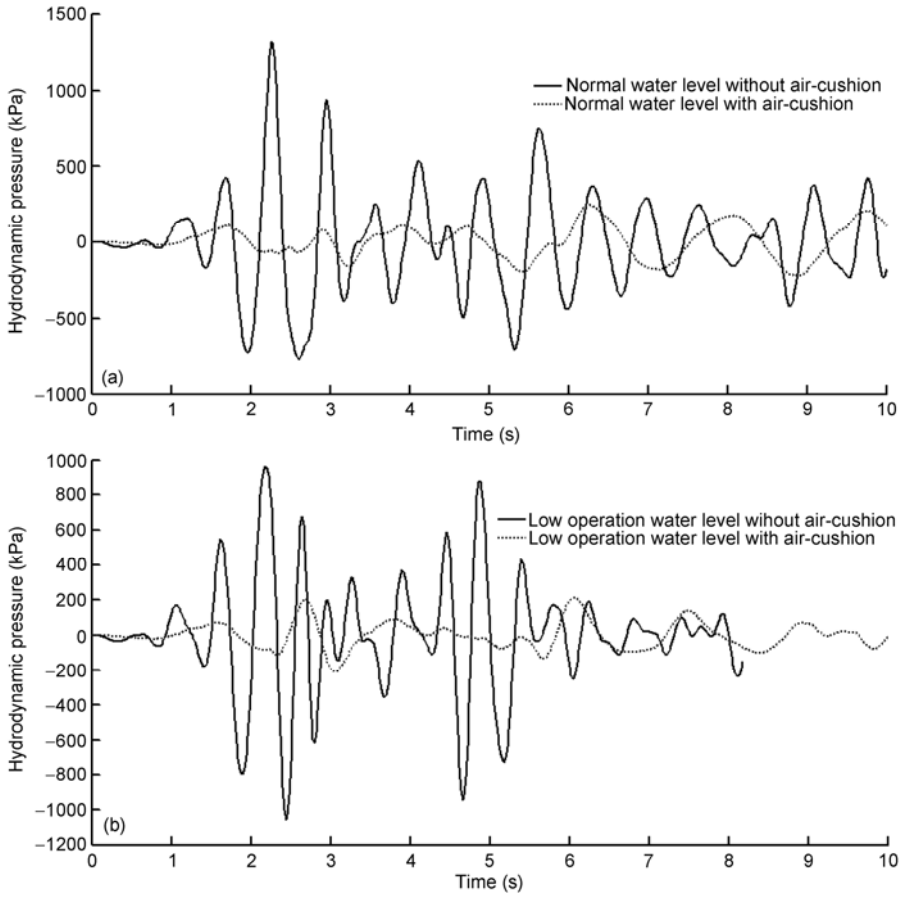

Figure 8 Time history of hydrodynamic pressures of Jinping high arch dam. (a) Normal water level; (b) low operation water level.

Table 4 Opening peak value (mm) of typical joint and its reduction range

Cases	II–1	II–2	II–3	II–4
Width of joint 5	23.47[a)]	8.64	24.22	18.58
Reduction range		63.2		23.3
Width of joint 7	11.6	9.60	37.80[a)]	23.30
Reduction range		40.4		38.4
Width of joint 10	28.44[b)]	7.92	39.80[b)]	28.11
Reduction range		72.2		29.4

Note: a), Second max value; b), max value of each joint.

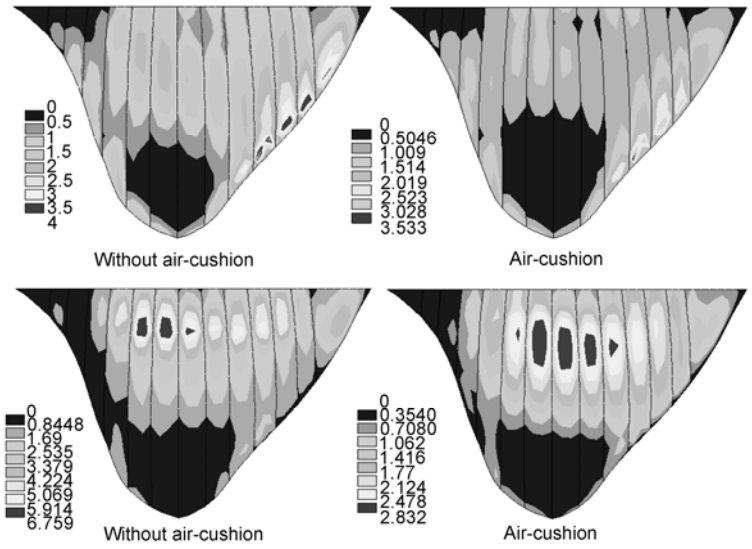

Figure 9 Maximum principal stresses plots on the upstream face of the dam (MPa).

Table 5 Peak hydrodynamic pressure (kPa) and its reduction range on the upstream face of the dam

Cases	II–1	II–2	II–3	II–4
Peak value of hydrodynamic pressure (kPa)	1332.2	262.2	963.5	245.9
Reduction range of hydrodynamic pressure (%)		80.2		74.5

Table 6 Peak value of the normal principal stress (MPa) and its reduction range

Cases / Stress type	II–1		II–2		II–3		II–4	
	Tens	Com	Tens	Com	Tens	Com	Tens	Com
Reduction rage (%)	4.39	14.91	3.53	–10.45	6.67	–19.29	2.83	–10.51
			19.6	70.1			58.1	45.5
Average reduction range (%)	38.8 (Tens. stress) / 57.8 (Com. stress)							

simulation method presented in this paper has been confirmed by the results of the numerical simulation of the practical arch dam.

2) The air-cushion has the excellent performance to reduce the hydrodynamic pressure, and the thicker the air-cushion is, the higher the reducing range is. When the average thickness of air-cushion is 2–3 m, the decreasing of the hydrodynamic pressure can reach to the order of 70%–80% during strong earthquakes. Moreover, this effect of decreasing hydrodynamic pressure is insensitive to the state (opening and closing) of the contraction joint opening or no-opening.

3) The reduction range of the opening width of the contraction joints shown in Table 4 can reach to the order of 40%–70% in the case of normal water level, and 20%–35% in low operation water level.

4) The reduction range of the principal stress shown in Tables 3 and 6 on the upstream face of the dam can reach to the order of 50% in the case of joint no-opening model, and 35%–55% in the case of the joint opening model. The decreasing amplitude of the principal stress can still reach to the order of magnitude of 20%–30% in consideration of the safety coefficient being 1.5–2. Undoubtedly, it has a significant contribution to the antiseismic safety of the high arch

dam.

5) The air-cushion isolation can directly decrease the earthquake loading, so it can not only improve the stress sate of the dam body but also enhance the whole-antiseismic capacity and safety of the dam engineering. This engineering measure is beneficial to the safety of dam body itself and the dam foundation-dam abutment. It is well known that the safety of the dam foundation and dam abutment are very important to the gravity dam and arch dam, respectively. Therefore, the air-cushion isolation should be the developing direction of the seismic catastrophe control for the high dams.

3 Optimization of air-cushion isolation control of high dam

3.1 Optimization of the air-cushion structure

The two arch dams engineering using air-cushion isolation mentioned above are the Chirkey and Miatly dams, USSR. Their air-chambers' structures of air-cushion are in the form of bell type, which is formed by hundreds of steel tubs in the way of turning over. Then, the material of the air-chamber was changed to the reinforced concrete and the hexagonal air chamber was used in the Mok gravity dam design shown in Figure 10.

The format of the entire air-cushion is firstly presented shown in Figure 11 to realize the optimum structure for the air-cushion. For each layer of the air-cushion, it is designed in the form of a gallery from a bank to another bank. The support plate between the air-cushion wall and the dam face is punched for aeration. All the improvements are to simplify the structure, construction and the gas supply pipeline by the greatest extent and to implement the spatial effect of isolation. In the air-cushion range, the volume ratio of the air can reach the order of 100%, which can guarantee the entirely separation of the dam body with the reservoir and maximize the isolated effect.

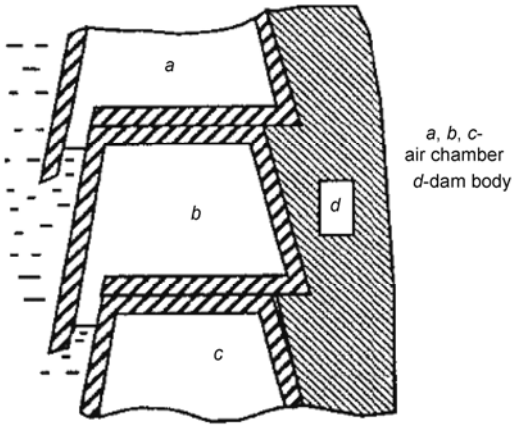

Figure 10 Section of the air-cushion of the Mok gravity dam in Russia.

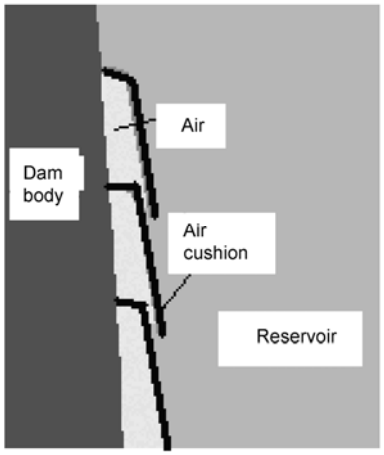

Figure 11 Scheme of the integral air-cushion.

3.2 Optimization of the air-cushion thickness

The air-cushion studied by the scholars in Russia and America was based on the assumption of constant thickness of the air-cushion. Obviously, it is not beneficial to the maximum of the isolated effect. The distribution pattern of the hydrodynamic pressure is that the deeper the water is, the bigger the hydrodynamic pressure is. Thus, the discrete optimization is adopted for the thickness and distribution of the air-cushion with the variable thickness along the height of the dam. Namely, the thickness of the air-cushion is thinner on upper dam face than that on the under part of the dam face. This form of the air-cushion is not only beneficial to strengthen the effect of the integral isolation but also save the engineering quantities of the air-cushion structure.

3.3 Engineering case of the high arch dam

In this paper, the three-stage discrete optimization is used as the optimization scheme of air-cushion for the Jinping high arch dam. This optimization scheme of air-cushion can be described as follow: the air-cushion with the thickness of 1 , 2 and 3 m is arranged on the upper, middle and under part of the upstream face of the dam, respectively. Namely, in the region of 0–80 m, 80–190 m and 190–300 m reservoir depth, the upstream face of the dam is covered by the air-cushion with the thickness of 1, 2 and 3 m, respectively. The total volume of this proposed scheme of the air-cushion is approximately the same as that scheme of the 2 m-constant thickness.

The dynamic-time history analysis for the above two proposed schemes (varied thickness, 2 m-constant thickness) of the air-cushion has been carried out. The results indicate that the optimized air-cushion has an advantage over the constant thickness air-cushion as follows.

• Decreasing of the hydrodynamic pressure—improving the efficiency of 1.9%–3.3%,

• Saving quantities of the air-cushion engineering—the

total volumes of the air-cushion of the schemes with varied thickness and 2 m-constant thickness are 142533, 153677 m^3, respectively, the reducing amplitude of the air volume can reach the order of 7.3%,

• Promoting efficiency of the air-cushion isolation—in summary, the efficiency of the unit volume of the air-cushion is promoted with the order of 9.9%.

4 Experimental verification of high dam's aseisimc aircushion control of large-scale shaking table tests

4.1 New type of dynamic similarity material of concrete and air-cushion material

The three control parameters of similar scale C for the dynamic model experiment are C_l, C_ρ, C_E, respectively, in which the subscript l, ρ and E identify the length, density and dynamic elastic modulus having $C_E = C_l \cdot C_\rho$. Usually, let C_ρ be 1, so the relation of $C_E = C_l$ need to be satisfied. However, the key problem is that the geometrical reducing scale of high arch dam is very large to make the dynamic elastic modulus of similar material to be very low, which is the difficult point. For this end, the digital-experimental system of MTS 815 is employed to develop the new type dynamic model material (DMM [21]) of concrete dams based on series of tests with hundreds of samples. The new type similar material, using the binder of rosin, has the chief advantages of high bulk density, low dynamic elastic modulus, distinct elastic deformation stage, and no toxic.

The quasi-dynamic 3D FEM analysis of the air chamber structure has been carried out. The tension tests of aluminum alloy sheets and ABS alloy sheets were performed. The ABS alloy sheets with 1 mm thickness were chosen as the model material of the air-chamber and the geometrical scale of air-cushion model for the dynamic experiment was satisfied.

Based on the above achievements, the large shaking table tests of the isolated dam model, which is satisfied with the basic dynamic similarity relations, were performed for the first time.

4.2 Experimental verification of high arch dam's aseismic air-cushion control of large shaking table dynamic model tests

The prototype used in this dynamic experiment model is Jinping high arch dam. The geometrical scale of the model is 1:300, the height of the model is 102 cm, the length, width of the dam foundation is 1.5, and 2.8 times the dam height, the length of reservoir is 3 times the dam height. The physical parameters of the experimental model are shown in Table 7.

Table 7 Physical parameters of dynamic experimental model

Material type	Bulk density (kN/m^3)	Dynamic elastic modulus (MPa)	Poisson's ratios
Dam body	24.0	425.6	0.27
Foundation	4.9	1300	0.16

The El Centro wave and 2008 Wenchuan-Shifang earthquake wave are taken as the input motion, the time-history analysis (calculated time is 0.75 s and time step 0.0005 s) of the dynamic experiment model has been performed, as well as the test model design and the test scheme.

The 6 m×6 m large-scale shaking table in the Nuclear Power Institute of China is used in the dynamic experiments. The main properties of this shaking table are that the scale of the shaking table is 6 m×6 m with six free degrees, the load capacity of the table is 60 t, its maximum acceleration at the direction of X, Y and Z is 1.0, 1.0, 0.8 g, respectively. The photo of the dynamic experiment model installed on the shaking table is shown in Figure 12.

Seeing that the main purpose of the tests is to check and verify the principle of the air cushion isolation; and the dynamic experiment of the liquid-gas-solid multi-field coupling is very complicated, the contraction joints are not arranged in this model test. After the completion of all the experimental tasks, by inspection, there is no any crack on the model.

18 cases including the models of with and without air cushion and different earthquake waves in the dynamic experiment are performed. Hydrodynamic pressure, as the typical experimental results, is the biggest concern. Figure 13 is both the distributions along the model dam height of hydrodynamic pressure of measured values and calculated values under the excitation of 2008 Wenchuan-Shifang earthquake wave.

The results show that the reduction ranges of the hydrodynamic pressure under the action of Wenchuan-Shifang earthquake wave is 77%, which are in relatively good agreement with simulation analysis of the dynamic experimental model. To sum up, for the first time performed have been the physical model experiment verification of the large

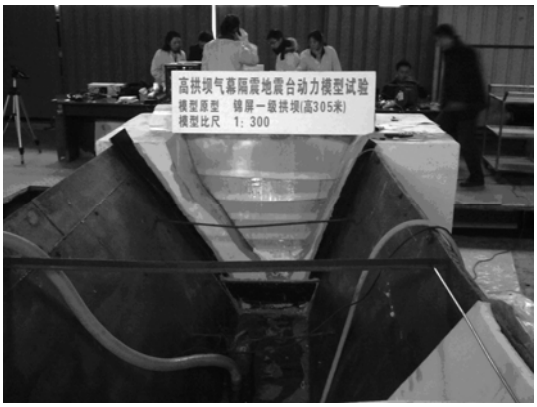

Figure 12 Photo of the experiment model on the shaking table.

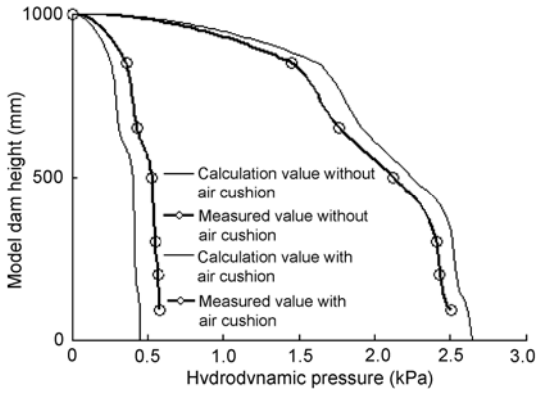

Figure 13 Distributions along the dam height of hydrodynamic pressure of measured values and calculated values.

shaking table tests, which are satisfied with the basic similarity criteria. The test data obtained and their distribution tendency and regularity are reasonable, and the results are trustworthy. Thereby, using the scientific experiment method of combination of physical model and numerical model, the powerful verification has been provided to the principle and technology of the air-cushion control of the high dams.

5 Conclusions

(i) The modeling theory and method of numerical implementation method of the liquid-gas-solid multi-field coupling simulation analysis of the air-cushion isolation control of the high arch dam have been presented for the first time. The theoretical description for the complicated dynamical problems of the tri-phase coupling—the thermodynamics state-material-contact/non-contact bi-nonlinearity, and the numerical simulation of key effects of dynamic catastrophe of the air-cushion isolation for the dam engineering have been put forward. The analytic solution for the simplification case of the rigid dam with plane wave has been created. The contrast simulation of the control to no-control of the seismic catastrophe process of 305 m Jinping high arch dam, highest in the world, has been performed. The analysis simulation results, whose regularity is good, are basically in agreement with the test data of the shaking table model and verify each other. Their basic results are rational and trustworthy worthy, and demonstrate the validity and effectiveness of the modeling theory and the numerical simulation method, and provide feasible media to research and design and calculation of aseismic control and air-cushion of high dams, as well as lay down a solid theory foundation for solving the key scientific problem of dynamic catastrophe control of high dams.

(ii) The entire air-chamber isolation and optimized air-cushion with varied-thickness are firstly presented. They are beneficial to reinforce the isolated effect and simplify the air-cushion structure. The optimization method of the dynamic control of high dams has been developed.

(iii) The large-scale shaking table dynamic model experiments of the air-cushion isolated arch dams, which are satisfied with the basically similar principle, have been firstly carried out. The measured data are reasonable and credible, and in basic agreement with the results obtained from the simulation analysis. So a powerful verification of model experiments has been provided to the theoretical model and the numerical method of the high dam's air-cushion control.

(iv) Using the experiment method of combination of numerical model and physical model, the mechanism and effects and optimization of high dams' air-cushion isolation have been systematically revealed and investigated. In the result, the effective breakthrough in the field of principle and technology of the air-cushion control of high dams has been achieved. The effectiveness of the hydrodynamic pressure reduction by using air-cushion of high arch dams has been verified to be certain and notable: when the thickness of the air-cushion is 2–3 m, the reduction range of the hydrodynamic pressure can reach to the order of 70%–80%; accordingly, the opening width of the contraction joints can be decreased significantly as well as the principal tensile and compressive stresses decreased for more than 20%–30%. The air-cushion isolation can not only safeguard the aseismic safety of the dam body, but also ensure the safety of the dam foundation and abutments, thereby enhance the antiseismic capacity and safety of the whole dam engineering. Therefore, the air-cushion isolation should be the prior developing direction of the aseismic control of the high concrete dams.

This work was supported by the National Natural Science Foundation of China (Grant No. 90715026).

1 Luo B Y, Xu Y J, Wang G L. Nonlinear dynamic analysis of Dagangshan arch dam with considering damper reinforcement (in Chinese). J Hydroelectr Eng, 2007, 26: 67–70
2 Wang H B, Li D Y. Aseismic Design of Arch Dam: Theory and Practice. Beijing: China Waterpower Press, 2006
3 ГеллисВ К, КАЛИЦЕВА И С, МЕЛЬНИКОВ Е П. Натурные иссления эксперименталъной воздушной завесы наплотине Кривопорожской ГЭС (in Russia). Гидротехническое строителъство, 1992, 10: 25–28
4 Боярский В М, МихАйлов Л П. Конструкцчия экспериментальной воздушной завесы для плотины Кривопорожской ГЭС (in Russia). Гидротехническое строителъство, 1992, 10: 11–13
5 Lombardo V N, Mikhailov L P, Semenov I V. Studies and design of earthquake resistant concrete dams. In: Proceedings of Inter Symposium on Earthquake and Dams. Beijing, 1987
6 ШЕЙНИН И С. Воздушная завеса для защнты гидротехнических сооружений от сейсмических и взрывных воздействий (in Russia). Гидротехническое строителъство, 1992, 10: 1–6
7 Hall J F, El-Aidi B. Hydrodynamic isolation of concrete dams. J Struct Eng, ASCE, 1987, 113: 1–10
8 Li L. A seismic isolation measure for dams. In: Proceedings of , 10WCEE-1992. Madrid, Spain, 1992

9 Xing J T, Zhou S, Cui E J. A survey on the fluid solid interaction mechanics (in Chinese). Adv Mech, 1997, 27: 19–38
10 He F X. Research of Hydrodynamic pressures on Arch Dams and Hydraulic Air-cushion Isolations. Dissertation of Doctoral Degree. Chengdu: Sichuan University, 2000
11 Wang Z. Research of Dam-Reservoir Interaction and Dam isolations Dissertation of Doctoral Degree. Chengdu: Sichuan University, 2001.
12 Long W F. Research on the Hydrodynamic Pressure and the Mechanisms of Air-cushion isolation of High-Dams. Dissertation of Doctoral Degree. Chengdu: Sichuan University, 2005
13 Zhang F. Dynamic Analysis and Experimental Research on the Mechanisms of Air-Cushion Isolation of Arch-dams. Dissertation of Doctoral Degree. Chengdu: Sichuan University, 2008
14 Liu H W, Chen J, Yang Z H, et al. Theory and numerical simulation of multi-field dynamic coupling of high arch dam seismic control (in Chinese). J Hydroelectr Eng, 2009, 28: 163–168
15 Chen J. Concentrated Seepage Monitoring Method Based on FBG for High Rick-fill Dams and Research of Air-cushion Isolation of High Arch Dams. Dissertation of Doctoral Degree. Chengdu: Sichuan University, 2009
16 Liu Y H, Zhang B Y, Chen H Q. Comparison of spring-viscous boundary with viscous boundary for arch dam seismic input model (in Chinese). Shuili Xuebao, 2006, 37: 857–862
17 Espandar E, Yazdchi M, Khahli N. Seismic analysis of arch dams—a continuum damage mechanics approach. Int J Number Methods Eng, 1999, 45: 1695–1724
18 Akköse M, Adanur S, Bayraktar A, et al. Elasto-plastic earthquake response of arch dams including fluid-structure interaction by the Lagrangian approach. Appl Math Modeling, 2008, 32: 2396–2412
19 Niwa A, Clough R W. Non-linear seismic response of arch dams. Earthquake Eng Struct Dyn, 1982, 10: 267–281
20 Chen H Q, Li D Y, Hu X, et al. Nonlinear model test and computation analysis on dynamic behaviour of arch dam with contraction joints (in Chinese). Earthquake Eng Eng Vib, 1995, 15: 10–15
21 Li Y, Zhang S J, Liu H W, et al. Experimental research on dynamic model material of high concrete dam (in Chinese). Rock Soil Mech, 2011, 32: 757–760
22 Zhang S J, Chen J, Zhang Y Z, et al. Isolation effect of air-cushion in high arch dams considering viscous-spring artificial boundary condition (in Chinese). Shuili Xuebao, 2011, 42: 238–244
23 Lin G, Hu Z Q. Studies of the effect of contraction joints and the effective earthquake-resistant measures for arch dams (in Chinese). World Earthquake Eng, 2004, 20: 1–8
24 Pan J W, Zhang C H, Wang J T, et al. Seismic damage-cracking analysis of arch dams using different earthquake input mechanisms. Sci China Ser E-Tech Sci, 2009, 52: 518–529